Postprint of: Mikielewicz D., Mikielewicz J., Analysis of Organic Rankine Cycle efficiency and vapor generator heat transfer surface in function of the reduced pressure, ENERGY Vol. 261 Part B (2022), 125329, DOI: 10.1016/j.energy.2022.125329

Analysis of Organic Rankine Cycle efficiency and vapor generator heat transfer area in function of the reduced pressure

Dariusz Mikielewicz [1], Jarosław Mikielewicz [2]

[1] Gdansk University of Technology, Faculty of Mechanical Engineering and Ship Technology

ul. Narutowicza 11/12, Gdansk, 80-233, Poland

E-mail Dariusz.Mikielewicz@pg.edu.pl

[2] Polish Academy of Science, Institute of Fluid-Flow Machinery

ul. Fiszera 14, 80-233 Gdansk, Poland

E-mail jarekm@imp.gda.pl

Abstract:

In the paper presented is analysis of the influence of reduced pressure on efficiency and heat transfer area of vapor generator of Organic Rankine Cycle (ORC) in case of subcritical and supercritical parameters of operation. Compared are two cases of subcritical and supercritical ORC featuring a similar arrangement of heat source supply and heat removal, that is featuring the same temperatures of working fluid before the turbine, and the same condensation temperature in the respective cycles. The analysis is helpful in selection of the appropriate

pressure in the vapor generator. In accomplished analyses a selection of wet ORC working fluids are scrutinized for a given range of heat source temperatures with respect to influence on efficiency of thermodynamic cycle and vapor generator area of heat transfer on installation and operation costs to illustrate the issue. Investment cost of a vapor generator in the ORC cycle accounts for a main share of expenditure alongside the cost of the expanding machine. Results of calculations show that from the point of view of cycle efficiency and size of vapor generator the pressures close to critical fluid pressure are usually optimal. Some working fluids feature even an optimal pressure. For the region close to critical point authors elaborated own method for heat transfer coefficients elaboration, which is useful in more exact estimations of heat transfer process in vapor generator. In case of a heat source with a relatively high temperature, it is better to consider a thermodynamic cycle with supercritical parameters even if as a result the vapor generator is slightly larger than for the case of a subcritical cycle. There will always be a more pronounced gain in efficiency compared to the expense induced by the heat transfer surface area of vapor generator.

Keywords: organic Rankine cycle, thermal efficiency, optimal boiling parameters, energy efficiency, thermodynamic cycle

NOMENCLATURE

c_p	–	specific heat, J/(kg K)
D	–	diameter, m
f	–	friction factor
F	–	channel cross-section area, m^2
g	–	acceleration due to gravity, m/s^2
G	–	mass flux, $kg/(m^2s)$

h – specific enthalpy, J/kg

h_{lv} – latent heat of evaporation, J/kg

L – tube length, m

$\dot{m}$ – mass flow rate, kg/s

N_T – turbine power, W

p – pressure, Pa

P – perimeter, m

$\dot{Q}$ – rate of heat, W

S – heat transfer surface, m^2

T – temperature, K

U_0 – overall heat transfer coefficient, $W/(m^2K)$

Greek symbols

α – heat transfer coefficient, $W/(m^2K)$

λ – thermal conductivity, W/(m K)

ρ – density, kg/m^3

μ – dynamic viscosity, Pa s

η_{th} – thermal efficiency

Subscripts

cr – critical point

crit – flow rate in critical cycle

exp – experimental

f – heating fluid

loss – thermal losses

m – mean value

opt – optimal

ORC – ORC

r – reduced parameter with respect to critical point value

rel – relative

0 – surroundings

1-10 – nodal points in thermodynamic cycle

Keywords: ORC efficiency, heat transfer close to critical point, heat exchanger sizing

1. Introduction

Recently proved shortages of gas and oil supplies together with the numerous countries commitments to stoppages of imports of such fuels from unsecure and non-democratic countries lead to further revisiting of the issue of green transformation [1]. In such light the deployment of technologies in generation of power utilizing industrial waste will attract even greater attention [2]. Due to the continuously increasing energy prices as well as their recent surge, it is becoming more and more economically profitable to recover even the low grade waste heat [3] and transform the waste heat into electricity. For this a most widely used solution is application of the organic Rankine cycle (ORC). In ORC installation the working fluid is an organic substance better suited than water to undergo phase changes at lower than 500^{o}C temperatures of the heat source [4,5]. Justification to use other than water working fluids is often due to the limited temperature level of the heat source, waste heat in particular. Temperature of the heat source is a major determinant of the type of technology required to

extract the heat and the uses to which it can be applied [6]. This puts a constraint on the maximum temperature and the evaporation pressure of the generated vapor in the ORC installation, and thus restricts the achievable electric efficiency of such power cycle. The low temperature heat source can either be of gaseous or liquid origin. Recently low temperature district heating networks attract the implementation of ORC [7-11], in which warm water is locally additionally heated using electricity or heat produced by the heat pump supplied by electricity produced by ORC. In case of ORC installation the investment cost is very important, as the cost of vapor generator and operational costs strongly influence the ORC efficiency. The vapor generator is an element of installation in which there are highest exergy losses. Appropriate design of ORC for such purpose requires careful techno-economic analysis to be conducted of such a cogeneration power station. In low-temperature systems there are large heat exchange surfaces required to extract required amount of energy. These factors emphasize the necessity of optimizing the cost effective design of power cycles.

It must be noted, that one of the important limitations in modelling of heat transfer in the vicinity of the thermodynamical critical point is the uncertainty related to thermophysical properties as one of the distinct features of heat transfer in that region. Small changes in temperature can lead to large changes in thermo-physical properties of the fluid [12,13] and subsequently influence the determination of heat transfer surface of vapor generator.

In literature there are numerous studies aiming at determination of the optimal temperature of evaporating fluid. Most of the studies are placing the objective function as maximum thermal efficiency or power output and are performed using advanced computational software. However there are also present some analytical approaches to establish optimal parameters of vapor generation. Even though the results of such analyses are still not presenting the consistent recommendations of best fluids and resulting temperatures of operation under specific temperatures of heat supply and removal from the ORC. The fluid which performs well under

some operation conditions not necessarily must be good at other ones. Tian et al [14] analysed 20 working fluids for recovering exhaust heat in IC engine using ORC. Employing a techno-economical model they found that system performance is better at higher evaporation pressures. R245fa has been recommended of the considered working fluids. Santos-Rodriguez et al. [15] considered uncertainty of determination of heat supply to obtain optimal operation conditions based on non-linear programming. Khennich and Galanis [16] considered the difference between the source temperature and the maximum working fluid temperature which maximize the thermal efficiency or minimize exergy losses, together with the total thermal conductance of the heat exchangers and turbine size. Optimum combinations of power and temperature differences were calculated for each one of these four objective functions. The ratio of total thermal conductance of the heat exchangers over the net power output indicated R141b as most suitable working fluid for the considered conditions. Ihuoma and Diemuodeke [17] considered optimal condensing temperature (OCT) of a subcritical ORC plant, where supplied heat is selected as the objective function. The wet fluids such as R717, methanol and ethanol have the potential of producing better thermodynamic figure of merit over the other fluid considered types. Igbong et al. [18] used exergoeconomic evaluation and optimization for geothermal energy utilization. Yu et al. [19] found that the profile of temperature-enthalpy of waste heat sources is usually not matching well the working fluid in ORC installation, hence effort should be exercised towards better matching of the profile of waste heat with the working fluid in ORC installation. In such case a higher evaporation temperature can be attained, which consequently leads to higher thermal efficiency of the system. Castelli et al. [20] considered exergy efficiency as a target function and found that the isobutane–isopentane mixture outperformed considered pure fluids of which RE347mcc is the best option. Balrse et al. [21] considered the constrained ORC design, i.e. a system featuring a fixed heat exchanger size and turbine configuration and compared the operation of working fluids. An energy and exergy analysis with the use of the

first and second law efficiency were applied. Non-constrained design favored working fluids with higher critical temperatures. Mikielewicz and Mikielewicz [22] considered the ratio of the heat exchanger area of the boiler to the power output is used as the objective function to determine the optimal boiling temperature for ORC installation. Evaporation temperature and inlet temperature of the heat source as well its mass flow rate are varied in the optimization method. Analysis led to a conclusions that relative power to ORC fluid flow rate with respect to evaporation temperature of working fluid exhibits a minimum at the optimal boiling temperature.

As stems from the presented literature survey there is still an open issue of appropriate selection of the boiling temperature on the performance and costs of the ORC installation. Additionally, the ratio of total thermal conductance of the heat exchangers over the net power output is a preliminary parameter, which can be used as a guidance techno-economic analysis.

In the paper is analysed the influence of boiling temperature in case of subcritical cycles or pseudocritical pressure in case of supercritical pressure cycle ORC on the cycle efficiency and dimensions of vapor generator. Compared cases of ORC have a similar arrangement of heat supply in the form of a single phase fluid and the same condensation temperature. The presented analysis should be helpful in selection of the appropriate pressure of heat supply for further techno-economic estimations of the total cost of power station and finally cost of electricity and heat produced.

2. Theoretical considerations

In the study both subcritical and supercritical cycles are analyzed. In both cases the working fluids which feature the end of expansion process in the wet vapor area are considered, namely they belong to the so called wet working fluids case [4].

2.1. Subcritical cycle

In case of subcritical cycle considered is a basic subcritical organic Rankine cycle operating under conditions close to the thermodynamic critical point, Fig. 1. The cycle is subsequently compared ~~with regard~~ to the hypothetical Rankine cycle with the line of critical pressure coinciding with the process of heat supply to the working fluid for expansion, see Fig. 2.

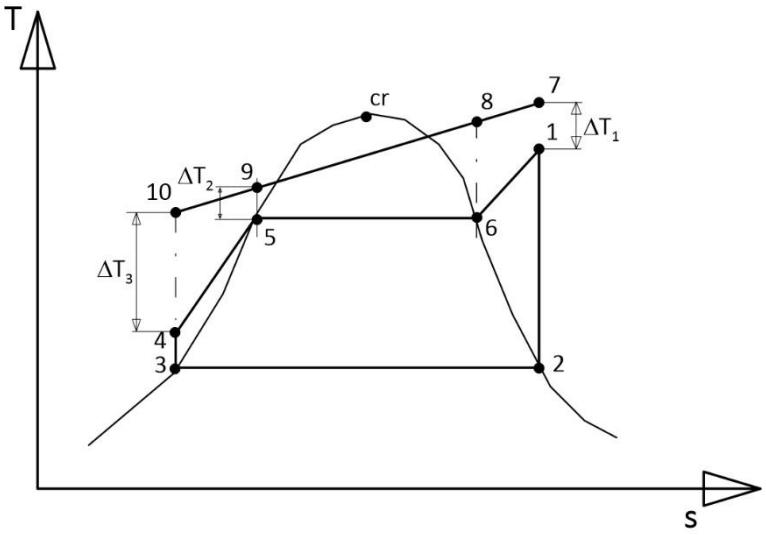

Figure 1. General schematic of a problem with constituent processes in the case of subcritical cycle.

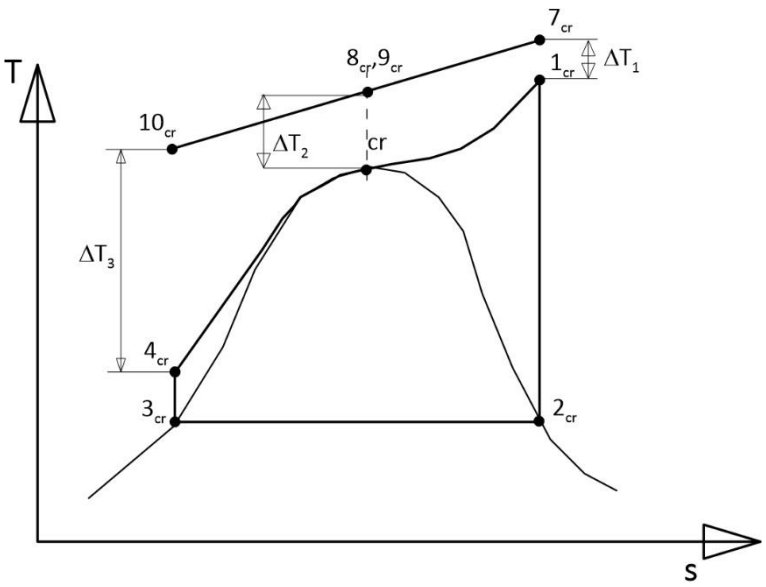

Figure 2. General schematic of a problem with processes of suppling heat in the case of a reference critical cycle.

The following assumptions are set in the study of subcritical cycle:

1. Considered is a thermodynamic cycle of a wet fluid, i.e. such one where the slope of the vapor saturation line is negative and the end of working fluid expansion is found in the two-phase region of T-s diagram. More precisely, the end of expansion coincides with the vapor saturation line at condensation pressure.
2. The maximum temperature of the heating fluid , T_7, is greater than the inlet temperature to the turbine, T_1, hence the temperature difference between the heat supply temperature and temperature of working fluid before the turbine is $\Delta T_1 = T_7 - T_1$.
3. The minimum temperature difference between the heat source and the ORC working fluid, the so called “pinch point” is equal to $\Delta T_2 = T_9 - T_5$.
4. The temperature difference between the heat source and the ORC working fluid at the end of heat supply process is equal to $\Delta T_3 = T_{10} - T_4$.
5. The heat supplying fluid is a single phase one, i.e. either liquid or gas. In the presented case the thermal oil is assumed as a heat source.
6. Condensation temperature T_c is constant in both subcritical and supercritical cycles, in calculations T_c =303 K was assumed.
7. In the study considered are cycles of with the same net power equal to 1 kW.
8. Overall heat transfer coefficient in vapor generator is assumed as a constant value being an average value in a particular zone, i.e. where the ORC working fluid is heated, then evaporated and last it is superheated.

The power produced by ORC is the difference between power of turbine and power of circulating pump and according to notation in Fig. 1 can be expressed as:

$$N_T = \dot{m}_{ORC}[(h_1 - h_2) - (h_4 - h_3)] \tag{1}$$

Balance of heat exchanged in the vapor generator from the inlet to the pinch point reads:

$$\dot{m}_f c_p (T_7 - T_9) = \dot{m}_{ORC}(h_1 - h_5) \tag{2}$$

The temperature of the heating fluid at pinch point can be determined from the condition of the set temperature difference at that location as:

$$T_9 = T_5 + \Delta T_2 \tag{3}$$

Mass flow rate of the heating fluid (thermal oil or other single phase fluid) circulating in the cycle can be calculated from equation (2) with the use of equation (1) to yield:

$$\dot{m}_f c_p (T_7 - T_{10}) = \frac{N_T}{[(h_1 - h_2) - (h_4 - h_3)]}(h_1 - h_5) \tag{4}$$

The outlet temperature of the heating fluid can be determined from the heat balance of vapor generator from the pinch point to the heating fluid outlet:

$$T_{10} = T_9 - \frac{(h_5 - h_4)}{c_p \frac{\dot{m}_{ORC}}{\dot{m}_f}} \tag{5}$$

The rate of heat supplied to the considered subcritical cycle yields:

$$\dot{Q} = \dot{m}_{ORC}[(h_5 - h_4) + h_{lv} + (h_1 - h_6)] \tag{6}$$

Due to the fact that in the vapor-generator there are three zones of heat transfer present,

namely the heat transfer between heating fluid (9-10) and single phase liquid (4-5), heating fluid (8-9) and two-phase evaporation (5-6), and finally heating fluid (7-8) and superheated vapor (6-1) the rate of heat supplied to the cycle can be expressed in terms of a product of overall heat transfer coefficient and a sum of a products of respective mean temperature differences in particular region and corresponding heat transfer surfaces, which is given as:

$$\dot{Q} = U_0\left(\Delta T_{m,1} S_1 + \Delta T_{m,2} S_2 + \Delta T_{m,3} S_3\right) \tag{7}$$

Mean temperature differences in the cycle are calculated approximately as:

$$\Delta T_{m,1} = \frac{(T_{10}-T_4)-(T_9-T_5)}{ln\left(\frac{(T_{10}-T_4)}{(T_9-T_5)}\right)} \approx \frac{(T_{10}-T_4)+(T_9-T_5)}{2} \tag{8}$$

$$\Delta T_{m,2} = \frac{(T_9-T_5)-(T_8-T_6)}{ln\left(\frac{(T_9-T_5)}{(T_8-T_6)}\right)} \approx \frac{(T_9-T_5)+(T_8-T_6)}{2} \tag{9}$$

$$\Delta T_{m,3} = \frac{(T_7-T_1)-(T_8-T_6)}{ln\left(\frac{(T_7-T_1)}{(T_8-T_6)}\right)} \approx \frac{(T_7-T_1)+(T_8-T_6)}{2} \tag{10}$$

Knowledge of respective mean temperature differences enables determination of the respective heat transfer surfaces of the vapor generator, namely S_1, S_2 and S_3, i.e. the surfaces where the ORC working fluid is respectively heated, then evaporated and last it is superheated.

$$S_1 = \frac{\dot{m}_{ORC}(h_5-h_4)}{U_0 \ \ \Delta T_{m,1}} \tag{11}$$

$$S_2 = \frac{\dot{m}_{ORC} \ \ h_{lv}}{U_0 \ \ \Delta T_{m,2}} \tag{12}$$

$$S_3 = \frac{\dot{m}_{ORC} \ \ (h_1-h_6)}{U_0 \ \ \Delta T_{m,3}} \tag{13}$$

Overall heat transfer coefficient is determined as for the tube.

2.2 Critical cycle as a reference cycle

As a next step, for the sake of subsequent comparative analysis and comparisons the reference

cycle, i.e. the critical thermodynamic cycle has been introduced. The course of the vapor generation coincides with the critical pressure isobar, whereas the heat supply line is above the critical pressure. The conditions of the end of expansion as well as these of the condensation temperature are the same as in the general subcritical thermodynamic cycle hitherto considered, i.e. states 2 and 3 are same for both cycles, hence $2=2_{cr}$ and $3=3_{cr}$. The difference is in the process 4_{cr}-1_{cr}, which in the case of the reference cycle coincides with the critical pressure isobar.

In line with Fig. 2, there can be distinguished two zones of heat supply in the vapor generator, i.e. heat supply process (10cr – 9cr) and receiving process for working fluid (4cr-cr) as well as heat supply line (9cr – 7 cr) and working fluid receiving line (cr-1cr). The rate of heat supplied to such reference cycle yields:

$$\dot{Q}_{cr} = \dot{m}_{ORC,cr}\left[c_{p,l}\left(T_{cr} - T_{4,cr}\right)+c_{p,g}\left(T_{1,cr} - T_{cr}\right)\right] \tag{14}$$

On the other hand the heat transfer to the cycle can be described by the heat transfer in two delineated earlier zones following relation:

$$\dot{Q}_{cr} = U_0\left(\Delta T_{m,1,cr}S_{1,cr} + \Delta T_{m,2,cr}S_{2,cr}\right) \tag{15}$$

Mean temperature differences in the reference cycle are calculated approximately as:

$$\Delta T_{m,1,cr} = \frac{\Delta T_1 - \Delta T_2}{ln\left(\frac{\Delta T_1}{\Delta T_2}\right)} \approx \frac{\left(T_{10,cr} - T_{4,cr}\right)+\left(T_{9,cr} - T_{cr}\right)}{2} \tag{16}$$

$$\Delta T_{m,2,cr} = \frac{\Delta T_2 - (T_9 - T_{10})}{ln\left(\frac{\Delta T_2}{(T_9 - T_{10})}\right)} \approx \frac{\left(T_{9,cr} - T_{cr}\right)+\left(T_{7,cr} - T_{1,cr}\right)}{2} \tag{17}$$

Knowledge of mean temperature differences, $\boldsymbol{\Delta T_{m,1,cr}}$ and $\boldsymbol{\Delta T_{m,2,cr}}$ enables determination of the respective heat transfer surfaces of the vapor generator:

$$S_{1,cr} = \frac{\dot{m}_{ORC,cr}\ \ c_{p,l}\left(T_{cr} - T_{4,cr}\right)}{U_0\ \ \Delta T_{m,1,cr}} \tag{18}$$

$$S_{2,cr} = \frac{\dot{m}_{ORC,cr}\ c_{p,g}(T_{1,cr} - T_{cr})}{U_0\ \Delta T_{m,2,cr}} \tag{19}$$

For the sake of subsequent comparisons we can also introduce the term expressing the ratio of total heat transfer surfaces in the subcritical ORC to the reference critical cycle:

$$S_{rel} = \frac{S_1 + S_2 + S_3}{S_{1,cr} + S_{2,cr}} \tag{20}$$

2.3. Supercritical cycle

A similar course of analysis can be accomplished for the case of supercritical cycle, Fig. 3. In such case the organic Rankine cycle considered is also a simple one operating under conditions above the thermodynamical critical point. The cycle is considered in reference to the same hypothetical critical Rankine cycle as in case of the subcritical cycle with critical pressure line coinciding with the working fluid heating process, see Fig 2.

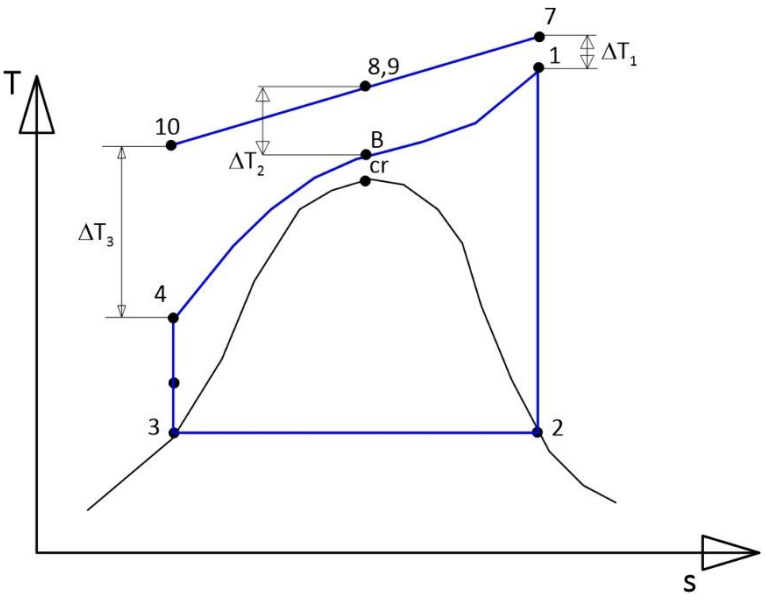

Figure 3. General schematic of a problem with the constituent processes in the case of supercritical cycle.

Similar assumptions as for subcritical cycle are made in the study of supercritical cycle except that:

1. The supercritical pressure of heated ORC fluid is n times higher than the critical pressure, i.e. $p_B=n\times p_{cr}$.
2. Overall heat transfer coefficient in vapor generator is assumed constant, because heat transfer coefficient of oil is much lower than that of working fluid ~~coefficient~~.
3. Temperatures $T_5=T_1+\Delta T_1$, $T_6=T_B+\Delta T_2$.

The similar algorithm of calculations of cycle efficiency and size of vapor generator heat transfer surfaces to the one presented for subcritical cycle is adopted to the supercritical cycle.

3. Results

The calculations for the considered cases have been accomplished using the Engineering Equation Solver software package [23], with appropriate cycle configurations procedures developed. As mentioned earlier in both cases of subcritical and supercritical cycles the same condensation temperature was applied, i.e. $T_c=303$ K. Three fluids have been selected for the analysis, namely R134a, R1233zd(E) and R290. Such selection of working fluids was dictated by the fact that R134a is a very well established fluid in contemporary refrigeration and heat pump applications, with some implementation cases in ORC. On the other hand R1233zd(E) is a representative of a new generation of synthetic fluoroolefines, HFO, whereas R290 is a natural fluid, recently quite often used in refrigeration technology. The precondition for selection of the fluid was that it belonged to the so called wet class of working fluids. It should also be stressed that presented here calculations are not aimed at selection of the best working fluid for operation in ORC but to present the capabilities of presented analytical approach. The values of temperature difference between the inlet temperature of heat source and temperature of working

fluid before the expansion device as well as temperature difference at the pinch point are set the same, i.e. $\Delta T_1 = \Delta T_2 = 10K$. The net power of the cycle has been assumed equal to N=1kW for all fluids. Calculated have been the values of thermal efficiency relative to the critical reference cycle efficiency, $\eta_{rel} = \eta_{th}/\eta_{crit}$, ratio of thermal oil flow rate to the ORC working fluid flowrate, $\dot{m}_{rel} = \dot{m}_f/\dot{m}_{ORC}$, relative heat transfer surface described by equation (20) and mean temperature differences determined using equations (8) to (10).

3.1. Subcritical cycle

The results of calculations for considered fluids in subcritical cycle are presented in Figures 4-9. The distributions of relative efficiency with respect to the reduced temperature, Fig. 4, show that in case of all considered fluids the value of unity is reached for approaching the critical point. The differences between values of efficiency for different fluids are small, whilst the R1233zd(E) exhibiting the biggest efficiency values and R290 the smallest of the ones considered. All thermal efficiencies increase with increasing reduced temperatures, $T_r = T_{evap}/T_{cr}$. In Fig. 5 presented is the ratio of thermal oil to ORC working fluid mass flow rates. In case of all fluids the ratio shows the decreasing trend with increase of reduced temperatures indicating at the same time that for higher reduced pressures a smaller amount of working fluid is required. The highest values of the ratio of flow rates is present for the case of R290 and the smallest one for R1233zd(E). The ratio of these two reaches a value of 4.25 for $T_r = 0.5$.

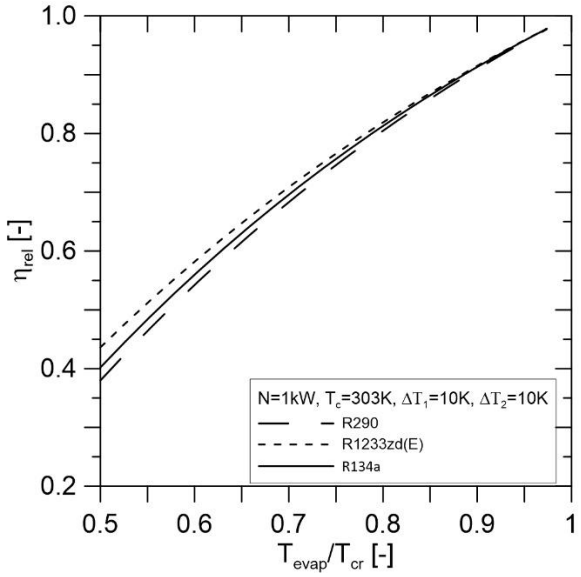

Figure 4. Relative efficiency in function of reduced temperature in the case of subcritical cycle; $\boldsymbol{\eta_{rel} = \eta/\eta_{cr}}$.

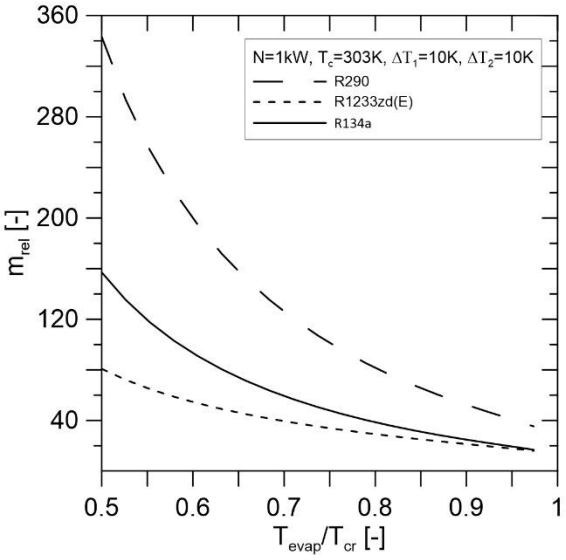

Figure 5. Ratio of thermal oil to working fluid flow rates in function of reduced temperature in the case of subcritical cycle.

In Fig. 6 presented are the distributions of the relative surfaces (described by equation (20)) for the case of considered fluids. The decreasing trend with increasing reduced temperature is primarily observed, however beyond the value of T_r>0.9 these ratios start to increase for R134a and R290, whereas in case of R1233zd(E) that increase starts at about T_r>0.8. One of the reasons for that is the fact that approaching thermodynamic critical point the mean temperature differences in definitions of surfaces S_2 and S_3 are becoming very small (see Fig. 8 and 9), which leads to significant increase in their values. The smallest mean temperature differences $\Delta T_{m,2}$ and $\Delta T_{m,3}$ are found for R1233zd(E), which confirms the reasoning. As the mean temperature differences are in denominators of the formulas (12) and (13) that leads to significant increase in the values of corresponding heat transfer surfaces. The smallest values of mean temperature differences $\Delta T_{m,2}$ and $\Delta T_{m,3}$ are found for R1233zd(E). In the case of that fluid a clear minimum in heat transfer surface is observed beyond which a significant increase in heat transfer surface is seen. Such distributions result from the course of distributions of

functions described by equations (11-13). In engineering practice temperature differences smaller than 1-2K are not advised due to the fact that the heat transfer surface are too excessive. Hence a conclusion, that too close operation of ORC to the thermodynamics critical point is not advised when the mean temperature difference between heat supply and working fluid is smaller than 1-2K. That is not the case for R134a and R290, however a slight increase in relative heat transfer surface is observed.

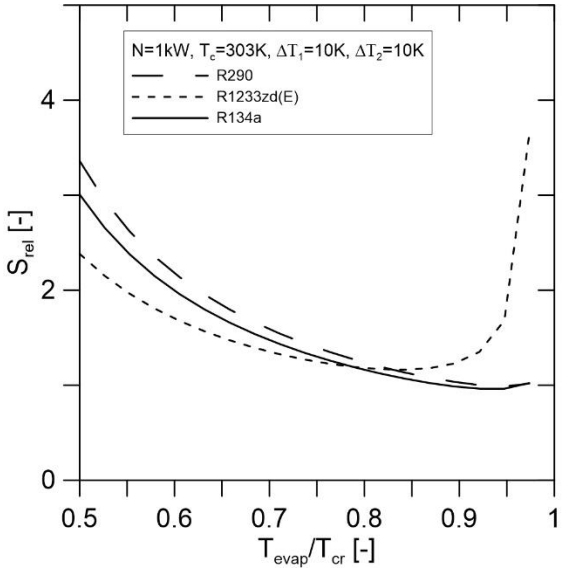

Figure 6. Ratio of heat transfer surface in the case of subcritical cycle to the heat transfer surface in the reference cycle in function of reduced temperature.

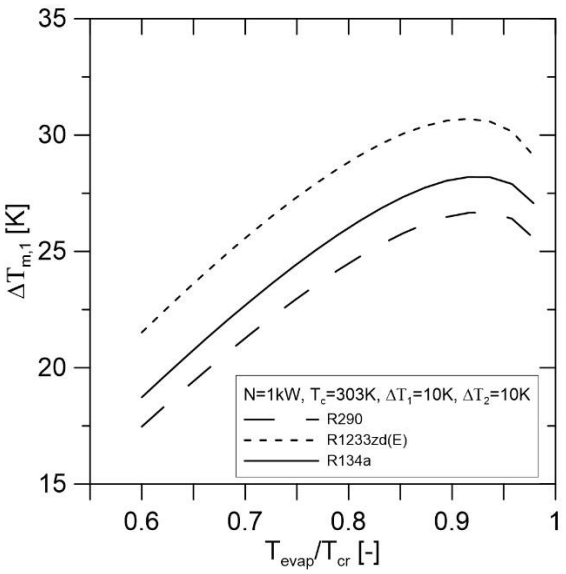

Figure 7. Mean temperature difference in the region of working fluid liquid heating in the case of subcritical cycle in function of

In case of heating of ORC liquid the largest values of mean temperature are found in case of R1233zd(E), whereas the smallest ones for R290. The maximum of the mean temperature can be observed at T_r=0.92. In the remaining two other regions of ORC fluid heating, namely the heating of two-phase fluid and heating of superheated vapor, respectively, there is a decreasing trend observed in mean temperatures in function of increasing T_r. The slope of changes for

larger values of T_r is greater than for the moderate values of T_r. The values of Δt_2 are tending to zero approaching the critical point as the latent heat of evaporation is tending to zero.

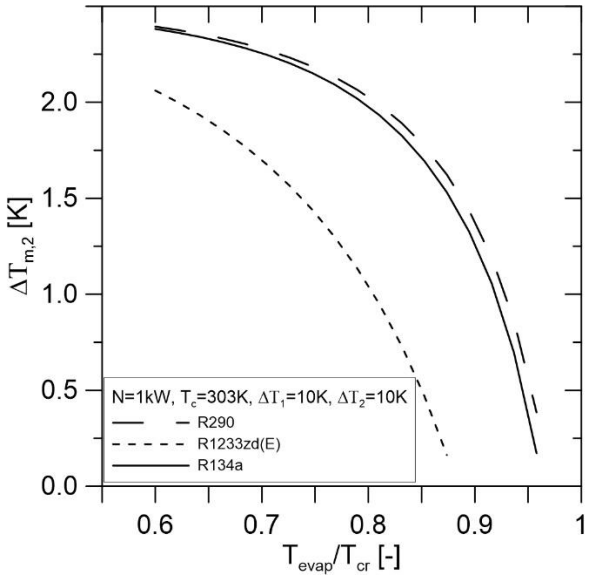

Figure 8. Mean temperature difference in the region of working fluid phase change in the case of subcritical cycle against reduced temperature

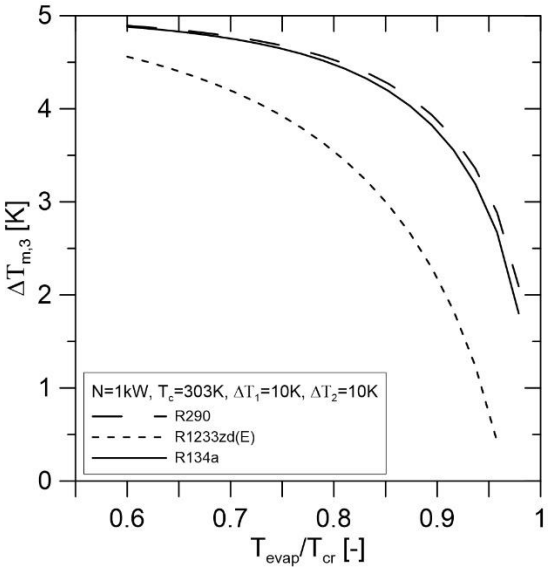

Figure 9. Mean temperature difference in the region of working fluid superheating in the case of subcritical cycle against reduced temperature

3.2 Supercritical cycle

The results of calculations for the supercritical conditions have been presented in Figures 10-13. Again, the distributions of relative cycle efficiency with respect to the critical reference cycle, the ratio of heating oil to ORC working fluid flow rates, relative heat transfer surface and the mean temperature difference with respect to T_1/T_{cr} temperature ratio are presented. In this case temperature prior to the expansion device T_1 has been selected, as that temperature is the highest in the cycle. In Fig. 10 values of relative efficiency exceeding unity are present due to the fact that the value of thermal efficiency for the supercritical cycle is higher than that of the reference critical cycle.

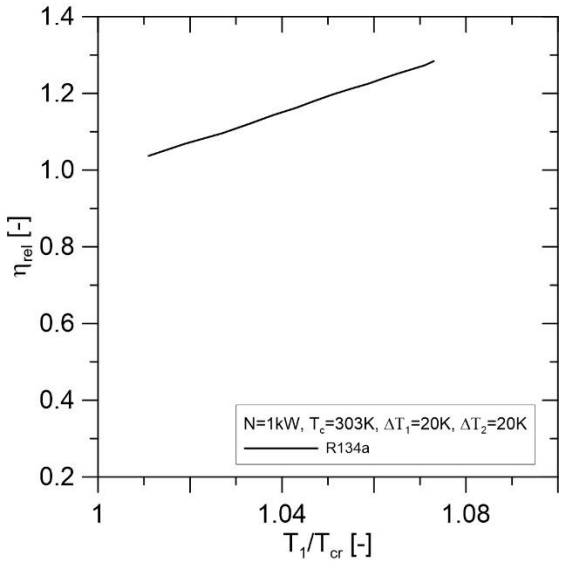

Figure 10. Relative efficiency in function of reduced temperature in the case of supercritical cycle; $\eta_{rel} = \eta/\eta_{cr}$ against reduced temperature

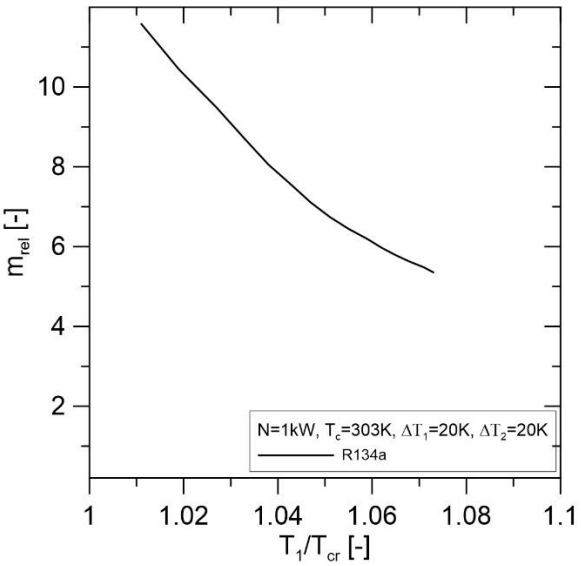

Figure 11. Ratio of thermal oil to working fluid flow rates in function of reduced temperature in the case of supercritical cycle. against reduced temperature

The value of relative efficiency increases with increasing of the turbine inlet temperature. In the case of the ratio of thermal oil to ORC working fluid flowrates that parameter strongly decreases with increase of the T_1/T_{cr} ratio. Next, attention is focused to the heat transfer surface in function of T_1/T_{cr} ratio in Fig. 12. An interesting minimum can be observed at the value of T_1/T_{cr} =1.032. However it can be said that changes of the surface with increasing temperature before the turbine are small overall.

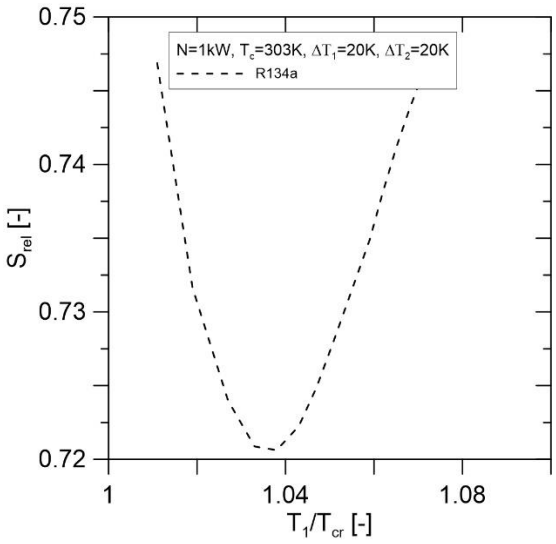

Figure12. Ratio of heat transfer surface in the case of supercritical cycle to the heat transfer surface in the reference cycle against reduced temperature

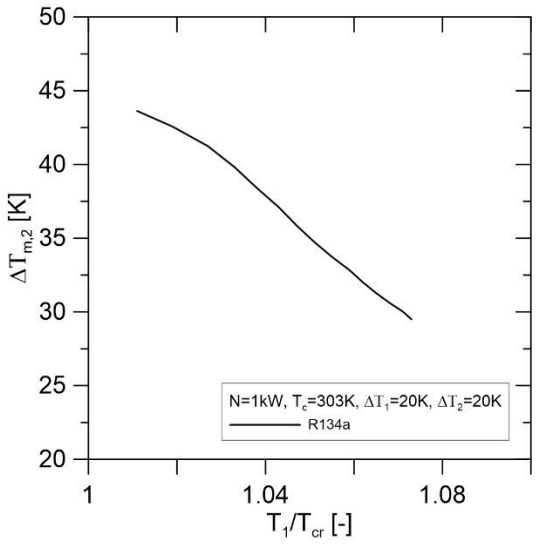

Figure 13. Mean temperature difference in the region of working fluid superheating in the case of supercritical cycle (nodes 5-6) against reduced temperature

3.4. Final remarks

Final analysis of the calculated values of performance of considered thermodynamical subcritical and supercritical cycles is presented in the form of heat transfer surface and the ratio mass flow rates of thermal oil to the ORC working fluid for both subcritical and supercritical conditions in function of the ratio of pressure against the critical pressure is shown in Figures 14 to 16. For the sake of comparisons a refrigerant R152a has been included into the analysis, which is considered as replacement to R134a and features a similar volumetric cooling capacity values. Its particular advantage is very low global warming potential (GWP = 124). Again, the purpose of considered fluids is merely to present the calculations to be obtained using a proposed model.

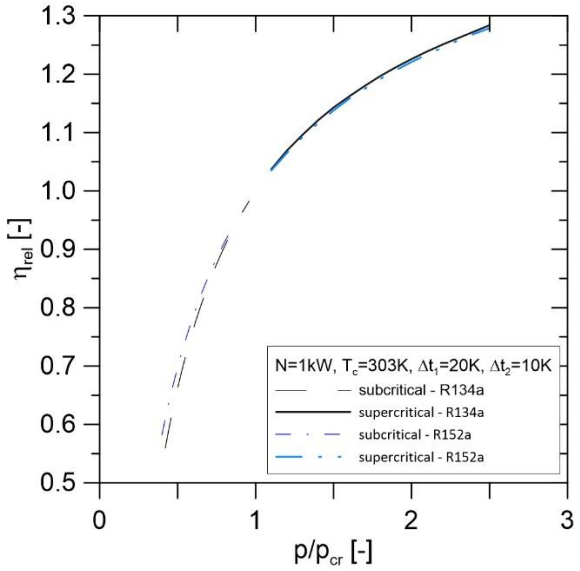

Figure 14. Relative efficiency ratio in the case of subcritical and supercritical cycles against reduced pressure

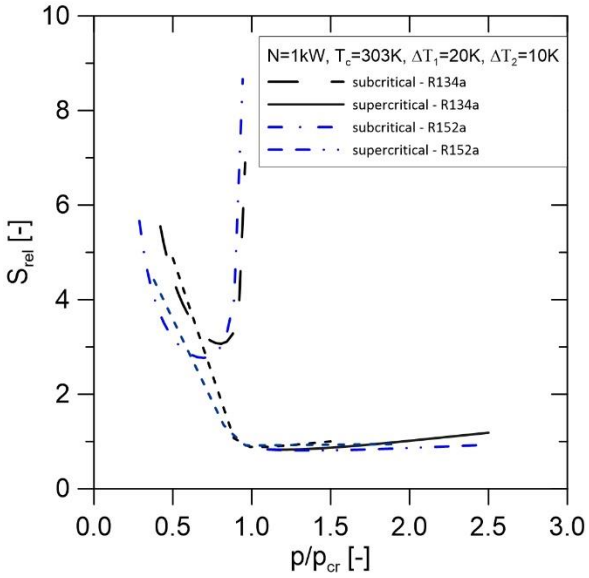

Figure 15. Ratio of heat transfer surface in the case of subcritical and supercritical cycles against reduced pressure

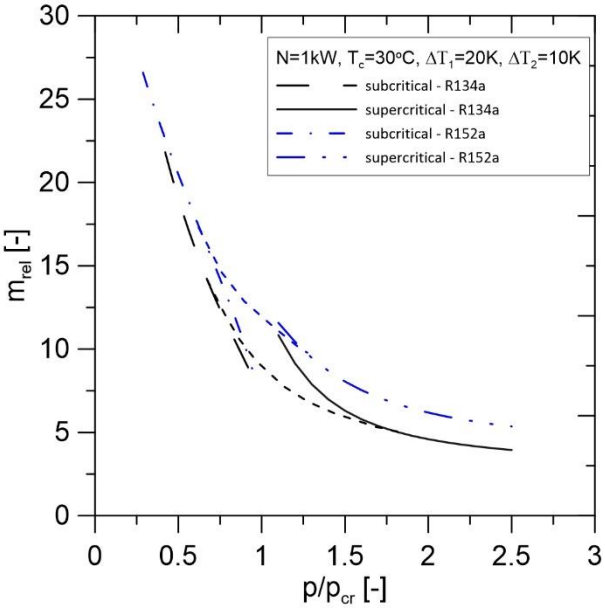

Figure 16. Relative mass flow ratio in the case of subcritical and supercritical cycles against reduced pressure

The relative efficiency exhibits a smooth continuous increase with the pressure ratio, which can be seen in Fig. 14. More peculiar distributions are obtained in the case of relative heat transfer surface, Fig. 15 and the ratio of thermal oil to ORC working fluid flowrates, Fig. 16. There is observed a discontinuity in distributions of relative heat transfer surface and the ratio of flow rates, which results from the application of relevant mathematical equations for their determination. In practice such discontinuities are not possible and hence there were introduced by authors dashed lines showing the probable behavior of the heat transfer surface and the mass flowrate ratio. The heat transfer coefficients for subcritical and supercritical conditions can be determined from authors own models for heat transfer coefficient determination developed earlier [25-28], whereas the overall heat transfer coefficients are calculated as for the case of tubes.

4. Conclusions

In the paper analysis of the efficiency, heat transfer surface and ratio of heating fluid to ORC working fluid have been considered. Introduced has been the reference critical thermodynamical cycle, to which the results of calculations have been compared. The models account for the conditions of the supply of heat to the cycle and the pinch point temperature difference in case of subcritical cycle.

In both cases it is observed that for increasing heat supply temperatures the cycle efficiency is increasing and the heat transfer surface is decreasing, similarly as the ratio of mass flow rates of thermal oil to ORC working fluid. Close to critical point the size of heat exchangers can be higher than for lower or higher temperatures. That is due to the fact that approaching thermodynamic critical point the mean temperature differences in definitions of surfaces S_2 and S_3 are becoming very small, which leads to significant increase in their values. In engineering

practice temperature differences smaller than 1-2K are not advised due to the fact that the heat transfer surface are too excessive. As high as attainable temperature and pressure of heat supply to the cycle seems to be most advantageous from the thermodynamic point of view.

If we have at our disposal a heat source with a relatively high temperature, it is better to consider a thermodynamic cycle with supercritical parameters even if as a result the steam generator is slightly larger than for a subcritical cycle. There will always be a more significant gain in efficiency compared to the expense induced by the heat transfer surface area.

Acknowledgments

Results presented in the paper have been carried out within the project 2017/25/B/ST8/00755 funded by the National Science Centre, Poland in years 2018-2021.

References

1. https://ec.europa.eu/info/strategy/priorities-2019-2024/european-green-deal_en
2. Directive of European Parliament 2010/75/UE of 24 November 2010 on industrial emissions, Official Journal of EU L334/17, 17.12.2010.
3. Mikielewicz D., Wajs J., Ziółkowski P., Mikielewicz J., Utilisation of waste heat from the power plant by use of the ORC aided with bleed steam and extra source of heat, Energy, 97, 11-19, 2016.
4. Mikielewicz J., Mikielewicz D., A thermodynamic criterion for selection of working fluid for subcritical and supercritical domestic micro CHP, Applied Thermal Engineering, Vol. 30, 2357-2362, 2010.
5. Pasetti M., Invernizzi C.M., Iora P., Thermal stability of working fluids for organic Rankine cycles: An improved survey method and experimental results for cyclopentane,

isopentane and n-butane, Applied Thermal Engineering, Volume 73, Issue 1, 2014, Pages 764-774, https://doi.org/10.1016/j.applthermaleng.2014.08.017.

6. Mikielewicz D., Mikielewicz J., Analytical method for calculation of heat source temperature drop for the Organic Rankine Cycle application, Applied Thermal Engineering, 63, 541-550, 2014.
7. Wang H., Wang H-Y, Zhu T., Gao N-P. Evaluation on energy performance in low temperature district heating system integrated with organic Rankine cycle, Appl Phys and Eng 2018 19(6) 481-478.
8. Yu H., Gundersen T., Feng X. Process integration of organic Rankine cycle (ORC) and heat pump for low temperature waste heat recovery, Energy 160 (2018) 330-340.
9. Ayub A., Invernizzi C.M., Di Marcoberardino G. Iora P., Manzolini, G., Carbon Dioxide Mixtures as Working Fluid for High-Temperature Heat Recovery: A Thermodynamic Comparison with Transcritical Organic Rankine Cycles. *Energies* **2020**, *13*, 4014.
10. Nasir M.T., Kim K.C., Working fluids selection and parametric optimization of an Organic Rankine Cycle coupled Vapor Compression Cycle (ORC-VCC) for air conditioning using low grade heat, Energy and Building, Vol. 129, 2016
11. Schmidt D, Kallert A., Blesl M., Svendsend S., Lid H., Nord N., Sipila K., Low Temperature District Heating for Future Energy Systems, Energy Procedia 116, 2017
12. Mikielewicz D., Mikielewicz J., Tesmar J., Improved semi-empirical method for determination of heat transfer coefficient in flow boiling in conventional and small diameter tubes. Int. J. Heat Mass Trans. 50(2007), 3949-3956.
13. Mikielewicz D., Mikielewicz J., Modelling of heat transfer in supercritical pressure recuperators, Energy, Vol. 207, (2020), 118251
14. Tian H., Shu G., Wei H., Liang X., Liu L., Fluids and parameters optimization for the organic Rankine cycles (ORCs) used in exhaust heat recovery of Internal Combustion

Engine (ICE), Energy, Volume 47, Issue 1, 2012, Pages 125-136, https://doi.org/10.1016/j.energy.2012.09.021.

15. Santos-Rodriguez M., Flores-Tlacuahuac M., Angel A., Gutierrez-Limon M., Lozano-Garcia F., Robust Optimal Design of Working Fluids for Sustainable Low Temperature Energy Recovery Under Uncertain Conditions, International Journal of Chemical Reactor Engineering, vol. 15, no. 6, 2017, pp. 20170091. https://doi.org/10.1515/ijcre-2017-0091
16. Khennich M., Galanis N., Optimal Design of ORC Systems with a Low-Temperature Heat Source, Entropy 2012, 14, 370-389; doi:10.3390/e14020370
17. Ihuoma U.V., Diemuodeke E.O., Optimal evaporating and condensing temperatures of organic Rankine cycle in a hot and humid environment, Nigerian Journal of Technology (NIJOTECH) Vol. 36, No. 1, January 2017, pp. 110 – 118, Faculty of Engineering, University of Nigeria, Nsukka, http://dx.doi.org/10.4314/njt.v36i1.14
18. Igbong D., Nyong O., Enyia J., Oluwadare B., Obhua M., Exergoeconomic Evaluation and Optimization of Dual Pressure Organic Rankine Cycle (ORC) for Geothermal Heat Source Utilization, Journal of Power and Energy Engineering, 2021, 9, 19-40, https://www.scirp.org/journal/jpee
19. Yu H., Gundersen T., Feng X., Process integration of organic Rankine cycle (ORC) and heat pump for low temperature waste heat recovery, Energy, Volume 160, 2018, Pages 330-340, https://doi.org/10.1016/j.energy.2018.07.028
20. Castelli A.F., Elsido C., Scaccabarozzi R., Nord L.O., Martelli E., Optimization of Organic Rankine Cycles for Waste Heat Recovery From Aluminum Production Plants, Frontiers in Energy Research, June 2019, Volume 7, Article 44, doi: 10.3389/fenrg.2019.00044
21. Barse K., Mann M., Maximizing ORC performance with optimal match of working fluid with system design (2016), Chemical Engineering Faculty Publications. 1. https://commons.und.edu/che-fac/1

22. Mikielewicz J., Mikielewicz D., Optimal boiling temperature for ORC installation, Archives of Thermodynamics, Vol. 33(2012), No. 3, 27–37, doi: 10.2478/v10173-012-0015-y
23. Engineering Equation Solver, F-Chart Software, Box 44042, Madison, WI 53744, USA.
24. Lemmon E.W., McLinden M.O., Huber M.L., NIST Standard Reference Database 23 Version, 10, National Institute of Standards and Technology, 2018.
25. Mikielewicz D., Mikielewicz J., A common method for calculation of flow boiling and flow condensation heat transfer coefficients in minichannels with account of nonadiabatic effects, Heat Tran. Eng., 32, 1173-1181, 2011.
26. Mikielewicz J., Mikielewicz D., A simplified energy dissipation based model of heat transfer for post –dryout flow boiling, Int. J. of Heat Mass Transfer 124 (2018) 260–268.
27. Mikielewicz J., Mikielewicz D., A simplified energy dissipation based model of heat transfer for subcooled flow boiling, Int . J. of Heat and Mass Transfer, 106, 280–288, 2017.
28. Mikielewicz D., Mikielewicz J., Modelling of heat transfer in supercritical pressure recuperators, Energy, Vol. 207, (2020), 118251